11-1-2009

Novel LC8 Mutations Have Disparate Effects on the Assembly and Stability of Flagellar Complexes

Pinfen Yang
Marquette University, pinfen.yang@marquette.edu

Chun Yang
Marquette University

Maureen Wirschell
Emory University

Stephanie Davis
Marquette University

Accepted version. This research was originally published in *Journal of Biological Chemistry*, Vol. 284, No. 45 (November 2009): 31412-31421. DOI.

Novel LC8 Mutations Have Disparate Effects on the Assembly and Stability of Flagellar Complexes*

Pinfen Yang[1,2]

Department of Biological Sciences, Marquette University
Milwaukee, WI

Chun Yang[1]

Department of Biological Sciences, Marquette University
Milwaukee, WI

Maureen Wirschell

Department of Cell Biology, Emory University
Atlanta, GA

Stephanie Davis

Department of Biological Sciences, Marquette University
Milwaukee, WI

LC8 functions as a dimer crucial for a variety of molecular motors and non-motor complexes. Emerging models, founded on structural studies, suggest that the LC8 dimer promotes the stability and refolding of dimeric target proteins in molecular complexes, and its interactions with selective target proteins, including dynein subunits, is regulated by LC8 phosphorylation, which is proposed to prevent LC8 dimerization. To test these hypotheses *in vivo*, we determine the impacts of two new LC8 mutations on the assembly and stability of defined LC8-containing complexes in *Chlamydomonas* flagella. The three types of dyneins and the radial spoke are disparately affected by dimeric LC8 with a C-terminal extension. The defects include the absence of specific subunits, complex instability, and reduced

Journal of Biological Chemistry, Vol. 284, No. 45 (November 2009): pg. 21412-31421. DOI.

incorporation into the axonemal super complex. Surprisingly, a phosphomimetic LC8 mutation, which is largely monomeric *in vitro*, is still dimeric *in vivo* and does not significantly change flagellar generation and motility. The differential defects in these flagellar complexes support the structural model and indicate that modulation of target proteins by LC8leads to the proper assembly of complexes and ultimately higher level complexes. Furthermore, the ability of flagellar complexes to incorporate the phosphomimetic LC8 protein and the modest defects observed in the phosphomimetic LC8 mutant suggest that LC8 phosphorylation is not an effective mechanism for regulating molecular complexes.

LC8 is an important component of vital complexes such as cytoplasmic dynein, myosin V, neuronal nitric-oxide synthase (1), and the nuclear pore complex (2). In *Chlamydomonas* flagella, LC8 is found in three types of dynein motors (the outer dynein arm (ODA),[3] the inner dynein arm (IDA) called the I1 dynein, and the cytoplasmic dynein motor CD1b for intraflagellar transport (IFT)) and in the radial spoke (RS) (3–7). The LC8-null mutant, *fla14,* has short, paralyzed flagella in which these complexes are absent or reduced (6) (Table 1). Drastic pleiotropic phenotypes also are noted in *Drosophila* LC8 mutants (8). In particular, the amorph mutant is embryonic lethal because of apoptotic death, consistent with the discovery that LC8 helps to sequester the pro-death apoptotic factor Bim (9).

Despite its significance, the function and regulation of LC8 are only partially understood. LC8 functions as a dimer with two identical binding sites for the target proteins (10, 11). One model postulates that the dimer tethers dynein motors to various cargoes (12). However, in some systems, the role of LC8 is unrelated to dynein motors (1, 13, 14). Another emerging model, founded upon structural analyses, contends that the bivalent structure of the LC8 dimer increases the stability (15) and promotes the refolding of the scaffold proteins in the complex (16).

Additional data indicate that LC8 is regulated by phosphorylation (17–19). The C-terminal Ser^{88} residue is phosphorylated in tumor cells, and the phosphorylation may promote cell survival by release and subsequent degradation of Bim (17). Consistent with this idea, a phosphomimetic LC8S88E mutant protein is predominantly monomeric *in vitro* and cannot bind to Bim or the target peptide from IC74 of cytoplasmic dynein (18, 19). However, LC8S88E does bind to peptides of Swallow, a target protein in the *Drosophila* oocyte (18). It was postulated that Swallow peptides have a stronger affinity for LC8 and bind to the small dimeric pool of LC8S88E, reversing the monomeric shift, and that LC8 phosphorylation is a selective regulatory mechanism. These observations raise a critical question about LC8 phosphorylation as a regulatory mechanism. How can phosphorylated LC8 promote cell survival while failing to bind vital target proteins, such as intermediate chains in cytoplasmic dynein? Testing these models for functional and regulatory mechanisms ultimately requires *in vivo* analyses.

In this study, we characterize the *Chlamydomonas* mutant *pf5* (20). The *PF5* gene product was implicated in integrating the assembly and function of axonemes because in addition to an RS deficiency and the lack of two minor RS proteins, RSP13 and RSP15, *pf5* axonemes also lack a small protein and an ∼110-kDa polypeptide of the inner dynein arms. The RS is part of a system that controls the activation of axonemal dynein motors. We discovered that the intriguing phenotype of *pf5* is actually caused by a mutation in the LC8 gene *FLA14*. This new mutant, expressing LC8 with a C-terminal extension (LC8CT), and an additional LC8 phosphomimetic mutant (LC8S90E) were used for analyses of the assembly and stability of the defined LC8-containing dyneins and the RS complexes in the *Chlamydomonas* flagellum (Table 1). Comparison of the phenotypes from these two new mutants and the LC8 null mutant (6) strongly support the predicted structural role of LC8 on target proteins to promote the stability and assembly of individual complexes at various levels. Furthermore, our results suggests that this function and molecular complexes are not significantly altered by LC8 phosphorylation.

Experimental Procedures

Strains and Culture Conditions

The following *Chlamydomonas* strains were used in this study: CC124 (WT mt—), CC1331 (*pf5 mt*—), and CC3937 (*fla14-1 mt*+). All strains were obtained from the *Chlamydomonas* Center (St. Paul, MN) and were cultured as described (21, 22) unless indicated otherwise.

The *fla14-1* strain was used for transformations with LC8 constructs (described below; see Table 1). Transformants used for this study include *fla14-LC8*, *fla14-LC8CT, fla14-LC8S^{90}A*, and *fla14-LC8S90E* (transformed with WT LC8, LC8CT, LC8S^{90}A, and LC8S90E constructs, respectively).

Molecular Biology, LC8 Genomic Constructs

The paromomycin resistance cassette was amplified from the pSI103 vector (21) and blunt-end cloned into the pBluescript vector at the SmaI site to generate the pPMM plasmid. Subsequently, LC8 genomic fragments, containing 0.55 and 1 kb of 5′- and 3′-flanking sequences (23) and the LC8 coding region, were PCR-amplified fromWTand CC1331 genomic DNA. The PCR products were cloned into the XhoI site in pPMM to generate pPMM-LC8 and pPMM-LC8CT plasmids.

For the LC8S90E phosphomimetic construct, PCR mutagenesis was performed to mutate the Ser^{90} codon (TCG) to a glutamate codon (GAA) using a primer containing the mutated sequence and a nearby BssHII restriction sequence. The PCR product was used to replace the equivalent fragment in the pPMM-LC8 plasmid to generate the pPMM-LC8S90E plasmid. For the LC8S90A construct, PCR-based site-directed mutagenesis was carried out using the QuickChange mutagenesis kit (Stratagene, La Jolla, CA).

Expression of His-tagged Recombinant Proteins

LC8 coding sequences were PCR-amplified and cloned into the NdeI and EcoRI sites of pET28(a) vector. The constructs were transformed into BL21(DE3) for expression as described (21). All constructs were confirmed by restriction digest and sequencing.

Genetics

Transformation rescue and genetic crosses were performed as described (21, 22). The experiments in which *fla14-1* was transformed with WT and mutant LC8 constructs allow for a direct comparison of the impacts of the LC8 mutations in an identical genetic background.

Biochemistry

Axoneme Isolation—Axoneme isolation, high salt extractions at 5 mg/ml and velocity sedimentation were carried out as described (21).

Analytical Gel Filtration Chromatography—Purified, recombinant LC8 proteins were dialyzed in 50 mM phosphate/citrate buffer, pH 3 or pH 7, for 24 h. 100-μl aliquots of 50 μM protein were fractionated on a Superose 12 HR 10/30 column with the dialysis buffer at a flow rate of 0.1 ml/min powered by an AKTA FPLC system.

Chemical Cross-linking—Isolated axonemes were treated with 1,5-difluoro-2,4-dinitrobenzene (Pierce) at a series of concentrations as described (10). After treatment, the axonemes were fixed for SDS-PAGE and analyzed by Western blots.

Antibodies—Antibodies were used in Western blots at 1:5000 dilutions to detect the following axonemal structures: for LC8 and the ODA, LC8 and IC78 (Dr. S. M. King, University of Connecticut Health Center) and IC69 (Dr. D. R. Mitchell, SUNY State Medical School); for I1 dynein, IC140, IC138, and IC97 (Dr. W. S. Sale, Emory University); for single-headed IDAs, p28 (Dr. G. Piperno, Mount Sinai Medical School); for the retrograde IFT motor CD1b, DLIC (Dr. M. E. Porter, University of Minnesota); and for the RS, RSP1 and RSP3 (Drs. D. R. Diener; J. L. Rosenbaum, Yale University) and RSP8, RSP11, and RSP16 (24).

Light Microscopy

Bright field light microscopy for motility assessment, imaging, and statistics was carried out as described (21). For flagellar length measurement, cells were fixed in 50% Lugol solution (Sigma). Images were magnified x2 optically and further enlarged x6 digitally. Flagella were traced on the monitor with a cotton thread, and the length was measured by a ruler. The measurement was converted to actual length by comparison with an image of a micrometer taken in parallel.

Journal of Biological Chemistry, Vol. 284, No. 45 (November 2009): pg. 21412-31421. DOI.

Results

pf5 Mutant Displays Multiple Flagellar Defects Because of a Mutation in the LC8 Gene—The *pf5* strain, CC1331, exhibits paralyzed or twitching flagella, typical for RS mutants with the occasional, slow swimming cell. We also found that these cells were defective in flagellar generation as well. Compared with the 10–12-μm WT flagella (Fig. 1*A*, *upper panel*), CC1331 flagella were about one-half length (Fig. 1*A*, *lower panel*; Table 1). Some cells have unequal length flagella (Fig. 1*A*, *arrowhead*) or flagella with swollen tips (Fig. 1*A*, *arrow* in *insets*), a phenotype typical of IFT mutants defective in the subunits of CD1b, the retrograde IFT motor, such as LC8 (6, 25).

To characterize the protein deficiencies in *pf5*, we performed Western blots of axonemes, probing for the subunits of the flagellar dyneins and the RS, structures that are crucial for flagellar motility and generation (Fig. 1*B*). As reported previously (20), compared with different loads of the WT control, the RS in *pf*5 axonemes, represented by RSP16 and RSP3, was reduced to ~50%, and the lower band for RSP3, indicative of the dephosphorylated form (26), was more prominent. The lack of RSP13 and RSP15 (20) was not further confirmed because antibodies to these RS subunits are not available. In contrast, the light intermediate chain (DLIC) of the retrograde IFT motor CD1b (25, 27), IC140 in I1 (28), p28 in single-headed IDAs (29), and IC78, LC6, and LC9 of the ODA (30) were not obviously affected. Interestingly, IC97 (also called IC110) in I1 (31) was not detectable, indicating IC97 is the missing 110-kDa IDA component in *pf*5 (20) and is not essential for the assembly of I1.

To determine whether the multiple defects observed in CC1331 were caused by a single mutation, the CC1331 strain was backcrossed to WT. The motility and axonemes of tetrads derived from 10 zygotes were analyzed. Segregation of the CC1331 motility phenotype was 2:2 with only parental di-types observed (10:0:0). As shown in the representative Western blots of axonemes (Fig. 2*A*), dephosphorylated RSP3 (*dot*), absence of IC97, and short twitching flagella (*T*) always co-segregated, whereas phosphorylated RSP3 and IC97 were only present in axonemes from 100%WTswimmers (*S*). The strict co-segregation of these biochemical markers and the motility anomaly suggested that the phenotypes are caused by a single mutation or tightly linked mutations.

To determine the genetic defect in *pf*5, transformation rescue experiments were carried out. CC1331 was co-transformed with BAC DNA that mapped near the *pf5* locus on linkage group III and a plasmid that confers paromomycin (PMM) resistance for selection. Only BAC DNA containing the LC8-encoding *FLA14* gene rescued the *pf5* mutant phenotype (data not shown). To determine whether *pf5* is defective in the LC8 gene, *FLA14* genomic DNA from CC1331 was amplified by PCR and sequenced. Two independent experiments showed that the TAA stop codon is replaced with the leucine-encoding TTA codon (*asterisk,* Fig. 2*B*) leading to an extended C terminus with an additional 23 amino acids, including 4 charged residues. The mutation is expected to result in a larger LC8 protein with a more basic pI than WT LC8. This result is consistent with the report that a small protein, presumably WT LC8, in the two-dimensional map of *pf5* axonemes was absent (20). Secondary structure analysis with the PHD program predicts that the addition also changes the conformation of the last β-strand (β*5,* Fig. 2*B*). As predicted, Western analysis showed that LC8 with the extended C terminus (LC8CT) was incorporated into CC1331 axonemes and is slightly larger than LC8 from WT axonemes (Fig. 2*C*).

To confirm that the CC1331 phenotypes were because of the read-through mutation in the LC8 gene, CC1331 cells were transformed with a single plasmid containing the WTLC8 gene (*FLA14*) and a paromomycin expression cassette for selection. The prediction is that the WT *FLA14* gene will rescue the flagellar length and motility defects in CC1331. Among 200 transformants, 86 clones were randomly selected for further analyses. Based on the motility, they were categorized into three groups: CC1331-like, WT-like, and mixed populations. Axonemes from each group were analyzed by Western blots (Fig. 2*D*). The CC1331-like clones (H7, H8, and G1) were immotile, had difficulty generating flagella (see low amounts of tubulin), and their axonemes still had high levels of dephosphorylated RSP3 (Fig. 2*D, dot*). Interestingly, axonemes from the transformants with swimmers contained both forms of LC8 (LC8CT andWTLC8). Those with only ~30% swimmers (A1, B12, and C10 strains) had more

LC8CT than WT LC8, whereas the strains with 100% swimmers contained largely WT LC8 (B11 strain) or a similar level of WT LC8 and LC8CT (B1 strain). Thus, LC8CT can compete withWTLC8 for assembly into the axoneme, and 50% WT LC8 is sufficient to restore WT-like motility. In the rescued strains, IC97 was restored, and RSP3 was largely phosphorylated. The varied ratio of WT LC8/LC8CT is likely because of different expression levels from the randomly inserted plasmid. CC1331-like transformants are likely because of the failed integration of theWTLC8 gene from the transforming plasmid.

Based on backcross, sequencing, and transformation rescue, we conclude that the read-through mutation of the LC8 gene results in the combined deficiencies in flagellar length (Fig. 1*A*) and multiple axonemal complexes, including IC97 in I1 (Fig. 1*B*). Therefore, CC1331 (designated as *pf5*) and *fla14* are defective in the same locus, and *pf5* is renamed as *fla14-3* after the two null mutants (6). Curiously, the *FLA14* gene from strain CC1028, which is listed as a *pf5* strain (*Chlamydomonas* Center), is normal and can rescue CC1331 phenotypes (data not shown). Thus, the paralysis of CC1028 is because of a mutation in a different locus.

In Vitro Analysis of Recombinant LC8 Variants—Structural analyses indicate the two C termini, including Ser^{88}, of the rat LC8 dimer are positioned in close proximity to the dimeric interface but not at the target binding sites (Fig. 3*A*). A phosphomimetic mutation in Ser^{88} (Fig. 3*A,* S88E; *yellow* residues with side chains) near the C terminus prevents dimerization *in vitro* because of charge repulsion, suggesting that phosphorylation is a mechanism for regulating LC8 by controlling dimer formation (18).

We postulate that the residues and charges in the additional C-terminal tail of *Chlamydomonas* LC8CT perturb dimerization leading to the severe phenotypes of the LC8CT strain (*fla14-3*). To test this, recombinant LC8, LC8CT, and LC8S90E (equivalent to S88E) were analyzed by gel filtration chromatography. As expected, at pH 7, WT LC8 was dimeric, and LC8S90E was largely monomeric (Fig. 3*B*). However, contrary to our hypothesis, recombinant LC8CT migrates as a slightly larger particle than WT LC8, indicating that LC8CT actually forms stable dimers. As expected, all LC8 constructs were monomeric at pH 3 because of protonation (16). Therefore, the deficiencies in LC8CT flagella are not because of a defect in its dimerization.

Effect of Phosphomimetic LC8S90E on Flagellar Complexes in Vivo—Because *Drosophila* phosphomimetic LC8S88E cannot bind IC74 of cytoplasmic dynein *in vitro*, we predict that the equivalent monomeric LC8S90E will result in severe deficiencies in the ODA, I1, and retrograde IFT. To test this, *fla14-1* was transformed with a plasmid expressing LC8S90E, WT LC8, LC8CT, or LC8S90A, a variant that cannot be phosphorylated (19).

More than 50 transformants for each construct were screened microscopically. As expected, theWTLC8 gene completely rescued the *fla14-1* phenotype (*fla14-LC8*), whereas the LC8CT transformants (*fla14-LC8CT*) resembled *fla14-3* (CC1331), with short, paralyzed flagella. Interestingly, *fla14-LC8CT* flagella were slightly longer than those of *fla14-1,* and both gradually shorten as time progressed (compare CT and null in Fig. 4*A*), even in the presence of WT levels of the retrograde motor (see *DLIC* in Fig. 1*B*). To our surprise, LC8S90E transformants (*fla14-S^{90}E*) appeared indistinguishable from WT LC8 strain in flagellar length (compare *LC8* and *S^{90}E*, Fig. 4*D*) and overall motility. A detailed analysis of three LC8S90E strains by high speed video microscopy (21) showed that their flagellar waveform was similar to WT LC8 strains, but the beat frequency was slightly slower (Table 1), a common trait of mutants with mild defects in the ODA (32).

To determine whether LC8S90E proteins were incorporated into the axoneme as monomers, isolated axonemes were treated with increasing concentrations of the short length cross-linker 1,5-difluoro-2,4-dinitrobenzene, which has been shown to cross-link axonemal LC8 dimers (10). Western blots showed that, in axonemes, LC8S90E was cross-linked into dimers as does WT LC8 (Fig. 4*B*), indicating that although LC8S90E is monomeric *in vitro*, it is incorporated into axonemes as a dimer *in vivo*.

To determine whether LC8S90E transformants exhibit any axonemal defects, axonemes with LC8S90E and WT LC8 were compared by Western blots. Interestingly, IC97 failed to assemble in

LC8S90E axonemes (Fig. 4*C*), a result similar to that observed in LC8CT axonemes (Fig. 1*B*). In addition, LC6 and LC9 from the ODA were reduced, a result that differed from LC8CT axonemes. The slight defect in ODA assembly is consistent with the slightly reduced beat frequency observed in these transformants (Table 1). However, in some preparations, these deficiencies were not as severe, suggesting variability in the assembly of these complexes in the LC8S90E strains. LC8S90A strains were indistinguishable from WT controls (data not shown).

Because of the varied severities in the LC8S90E phenotype, we tested if the deficiency could be enhanced by culturing cells in adverse conditions, on agar plates in a dim-lighted room at 32°C for 14 days followed by resuspension in water at 32°C. All strains were assessed as percentage swimmers at three time points after resuspension. Under these conditions, the *fla14-1* and *fla14-LC8CT* strains were entirely immotile, and most cells lacked flagella (Fig. 4*D*, *fla14-1* and *LC8CT*). Although fast swimmers were noted in the *fla14-LC8* and *fla14-S90A* strains after 30 min, only ~10–50% cells swam in 3.5 h (Fig. 4*D*, *WT* and $S^{90}A$), indicating the culture condition was not favorable for flagellar generation. Importantly, the LC8S90E swimmers did not appear until 3.5 h (Fig. 4*D*, $S^{90}E$), and the movement was sluggish. Together, these results indicate that LC8S90E affects the ODA more severely than other flagellar complexes. The deficiency becomes more severe and extends to other flagellar complexes when cells are grown in challenging conditions. As additional controls, LC8S90E cells grown in 32 or 24°C growth chambers with bright light and controlled humidity appear normal (data not shown), indicating the enhanced phenotype of LC8S90E is not merely because of temperature sensitivity.

Dissociation of Axonemal Dyneins and RS Complexes in LC8 Mutants—To test if the mutant LC8 molecules affect the stability of flagellar complexes, axonemal dyneins were extracted by 0.6 M NaCl followed by velocity sedimentation in 5–20% sucrose gradients and Western blot analyses (Fig. 5*A*). As anticipated for WT, the ODA and I1 sedimented as intact ~20 S particles (represented by IC78 and IC140, respectively), and LC8 primarily co-sedimented with the abundant ODA. In the *fla14-LC8CT* strain, the ODA remained at ~20 S. In contrast, IC140 sedimented as a smaller particle, at a position similar to p28 (Fig. 5*A, arrow*) in single-headed dyneins, and IC138 was found in multiple peaks, indicating the I1 complex is less stable and dissociates upon extraction. Interestingly, in the LC8S90E gradient, even though IC97 was absent, I1 did not dissociate, whereas the ODA did (Fig. 5*A, IC78* and *IC69*). In this case, IC78 sedimented closer to the top of the gradient, although IC69 sedimented at a position similar to IC140 in the LC8CT gradient. Thus, I1 is more sensitive to LC8CT, although the ODA is more sensitive to LC8S90E. Because CD1b dissociates readily under these conditions (27), the stability of this complex was not assessed.

To test the effect of the LC8 mutations on the stability of the RS complexes, axonemes were extracted with 0.5 M KI and then fractionated similarly. As shown by RSP16 Western blot, the RSs sedimented as intact 20 S particles (Fig. 5*B*). In contrast, in LC8CT extracts, all RSPs tested, including RSP16 and four other RSPs that are located at different subdomains of the RS complex (24), sedimented near the top of the gradient, indicating a drastic disintegration of the RS. Therefore, LC8CT interferes with the assembly of individual RS complexes, phosphorylation of RSP3, and the incorporation of the RS into axonemes (Fig. 1*B* and Fig. 5*B*).

Discussion

The major challenges in understanding LC8 function are the severe pleiotropic phenotypes of the previously described LC8 mutants and the lack of *in vivo* context in the simplified *in vitro* systems. These constraints are overcome by the two new LC8 mutants and the *Chlamydomonas* experimental system with defined LC8-containing complexes. The key results are that phosphomimetic LC8S90E, although monomeric *in vitro*, is a dimer *in vivo* and only causes minor defects. In contrast, dimeric LC8CT results in disparate assembly deficiencies and the dissociation of complexes that are otherwise rather stable. These results support the proposed structural role of LC8 in forming a core scaffold (15, 16) and shed new light on the regulation and ultimate function of LC8.

LC8 Promotes the Formation of the Retrograde IFT Motor for the Generation of Full-length Flagella—Because the transient short flagella of *fla14-1* lack retrograde IFT and the responsible motor CD1b, it was postulated that retrograde IFT recycled the IFT machinery for flagellar generation and maintenance, and thus *fla14* generated short flagella that resorb prematurely because of depleted IFT rafts (6). Yet defects in multiple axonemal complexes in *fla14-1* could result in short flagella (29). The IFT deficiency model was confirmed by *fla14-3* (LC8CT strain) that also displayed a similar length phenotype but milder axonemal defects that are insufficient to affect flagellar length. Interestingly, the amount of DLIC appears normal in LC8CT flagella (Fig. 1*B*) indicating that the retrograde IFT motor can enter flagella, but its function is still impaired. Importantly, the defects in the IFT motor and axonemal complexes appear independent.

LC8 Directly Promotes the Proper Assembly of Individual Complexes at Multiple Levels—One theory proposes that numerous LC8 target proteins are the cargoes of dynein motors and that the bivalent LC8 dimers adhere the motors and the cargoes together. This idea is consistent with the deficiencies of the LC8 null flagella in which the retrograde IFT motor, CD1b, is absent and its putative axonemal cargoes are reduced or absent. However, defective motorcargo coupling cannot explain the defects in LC8CT-containing flagella in which retrograde IFT is dysfunctional, although the ODA appears largely normal; the RS is unstable (Fig. 5*B*) and poorly incorporated into axonemes, and I1 is only missing a single subunit (20) (Fig. 1), and it dissociates upon extraction (Fig. 5*A*). Such disparate structural deficiencies in the four flagellar complexes are indicative of individual assembly defects and strongly suggest that LC8, normal or mutated, is in a critical position in each flagellar complex to directly affect the assembly unique to each complex.

These deficiencies can be partially explained by the model that the LC8 dimer stabilizes or refolds dimeric scaffold molecules in molecular complexes (15, 16). It is conceivable that the LC8 dimer associates with putative scaffold proteins, such as WD-repeat ICs in dyneins (30) (Fig. 6, *left*) and unknown proteins in the RS. This binding can enhance the stability of dimeric scaffold proteins and transform the flanking disordered regions into a conformation that favors the association with additional molecules, such as IC97 in I1, the LCs in the ODA (Fig. 4), RSP13/15 in the RS (20), IFT particle proteins in the case of CD1b, or docking proteins responsible for anchoring axonemal complexes. Thus, through modulation of target proteins, LC8 promotes the assembly of various complexes and higher level complexes. When LC8 is mutated, such as LC8CT, the additional sequence (Fig. 6, *right, red triangles*) at the dimeric interface may act as a wedge that alters the dimeric conformation or creates steric hindrance, consequently reducing the stability of the complex and interfering with further interactions.

As instrumental and important as LC8 is, it is critical to attribute its contribution objectively to understand the grander scheme of molecular assembly. Contrary to the prediction (33), LC8 is not necessary for initiating assembly and may not be involved in the initiation process at all. Studies of *fla14-1* showed that without LC8, flagellar LC8 complexes actually assemble, although the process is defective at different steps for each complex. For example, the subunits of CD1b are dispersed in the cell body of a DLIC mutant (25, 27, 34), indicating that this subunit is essential for assembly of the retrograde IFT motor. In contrast, in WT and the LC8 null mutant (*fla14-1*), the other subunits of CD1b are concentrated around the peribasal body region. Thus, in the absence of LC8, the retrograde IFT motor is assembled into a defective complex that cannot enter flagella. In the case of the RS, the precursor RS complex enters flagella (26) but cannot be incorporated into axonemes, resulting in the absence of RS structures in *fla14-1* axonemes. I1 is assembled in *fla14-1* axonemes, although it is less abundant (6). Thus, the modulation of target proteins by LC8 is to correctly promote further assembly rather than to initiate the assembly of complexes.

The unique subunits in I1 also caution the strict interpretation that LC8 target proteins only function as molecular scaffolds (16). The actual target proteins of LC8 in I1 have not been determined. However, neither IC138, a candidate scaffold molecule with WD repeats, nor IC97, which is most sensitive to the LC8 mutations, is required for I1 assembly (31, 35). Instead, both are implicated in phosphoregulation of I1 (31, 35, 36). These unique subunits explain the less severe defects of I1 in *fla14-1* and demonstrate the varied roles of LC8 target proteins.

Differential Accommodation of Mutated LC8—The scaffold model portrays LC8 actively refolding target proteins (16). This study shows the individual ability of each flagellar complex to accommodate the modified LC8 molecules. For example, the ODA accommodates LC8CT better than LC8S90E, whereas the other complexes accommodate LC8S90E better than LC8CT.

Two possibilities can explain these differences. Despite a common LC8-binding motif (37, 38), the actual LC8-binding sequences are longer and rather diverged (11) and may have different affinity for mutated LC8 proteins. Furthermore, the molecular context of each LC8 complex, which cannot be tested *in vitro*, may influence how severe a particular complex will be affected by each LC8 mutation. For example, it was postulated that five tightly packed LC8 dimers promote the folding of the dimeric scaffold proteins in the yeast nuclear pore complex (2). Similarly, two LC8-binding sites are immediately adjacent to each other in the WD repeat subunit of CD1b (34) that is particularly sensitive to LC8CT. It is conceivable that multiple tightly packed LC8CT dimers with additional tails will amplify the impact on the target proteins and complexes.

In contrast, the target proteins and neighboring subunits of each complex, which are also involved in assembly of the scaffold (15, 30, 39), may contribute to the ability of each complex in accommodating a particular LC8 mutation, particularly the phosphomimetic LC8 that is inherently monomeric *in vitro* (Fig. 3), thus reducing or eliminating the impact of modified LC8.

Limited Effects of LC8 Phosphoregulation—It has been proposed that LC8 phosphorylation is a selective regulatory mechanism (18). The subtle phenotype in the LC8S90E phosphomimetic mutants suggests that the phospho-regulation is more restricted than anticipated. One idea is that LC8 phosphorylation induces a monomeric shift that preferentially interferes with the binding of lower affinitive target proteins, such as the intermediate chain target peptides from *Drosophila* dynein (18). Consistently, the ODA and I1 in

Chlamydomonas flagellar are abnormal (this study). However, the important differences are that the flagellar dyneins incorporate LC8S90E as dimers (Fig. 4*B*), and the defects are insufficient to cause obvious functional deficiencies in *Chlamydomonas* flagella in standard laboratory growth conditions (Fig. 4*A*). Although the phosphomimetic mutation is not identical to phosphorylation, these modest effects from LC8S90E raise doubts on the effectiveness of LC8 phosphorylation in regulating flagellar functions and molecular complexes in general. In fact, to date, we have not been able to identify phosphorylated LC8 in *Chlamydomonas* flagella (data not shown). The strains with LC8S90A that cannot be phosphorylated appear normal as well. This tolerance of phosphorylated LC8 by most complexes could be advantageous such that phosphorylated LC8 could primarily affect a small number of target proteins, like apoptotic factor, to promote cell survival (17, 19) without causing deleterious side effects such as the disruption of dynein motors.

The enhanced phenotypes of the phosphomimetic mutants in adverse conditions suggest that the conserved Ser^{90} is important but not for phosphorylation. The deficiency of S90E flagella became more severe under dimmer light and warmer growth condition that even challenges WT (Fig. 4*D*) but is not unusual in natural habitats. Yet it is under this condition that the difference between WT and the phosphomimetic mutant becomes evident. Perhaps the phosphomimetic LC8 is less effective in promoting assembly. The inefficiency is masked under ideal laboratory conditions but becomes apparent in challenging situations in which myriads of cellular reactions, such as protein synthesis, are critically reduced. As shown in a structural study, the hydroxyl group of Ser^{88} at the interface may contribute a hydrogen bond (18) that favors the dimerization to effectively promote the proper assembly of molecular complexes under diverse conditions.

As small as LC8 is, it has been assigned an accolade of titles. By taking advantage of *Chlamydomonas* mutants and the well characterized LC8-containing flagellar complexes, this study has provided the critical *in vivo* evidence and the molecular context to substantiate the structural model for LC8 function, further revealing the ultimate function for LC8 in fostering the proper assembly of flagellar complexes and the limit of postulated phosphoregulation. These conclusions are likely applicable to diverse complexes as well as higher level complexes that contain LC8 in other systems (40, 41).

Acknowledgments

We are grateful for the mutant strains and the meticulous records provided by Dr. Elizabeth Harris at the Chlamydomonas Center and for antibodies generously provided by Drs. S. M. King (University of Connecticut Health Center), D. R. Mitchell (SUNY Upstate Medical University), W. S. Sale (Emory University), G. Piperno (Mount Sinai Medical School), M. E. Porter (University of Minnesota), and D. R. Diener and J. L. Rosenbaum (Yale University).

References

1. Pfister, K. K., Shah, P. R., Hummerich, H., Russ, A., Cotton, J., Annuar, A. A., King, S. M., and Fisher, E. M. (2006) *PLoS Genet.* 2, e1

2. Stelter, P., Kunze, R., Flemming, D., Ho¨pfner, D., Diepholz, M., Philippsen, P., Bo¨ttcher, B., and Hurt, E. (2007) *Nat. Cell Biol.* 9, 788–796

3. Piperno, G., and Luck, D. J. (1979) *J. Biol. Chem.* 254, 3084–3090

4. King, S. M., and Patel-King, R. S. (1995) *J. Biol. Chem.* 270, 11445–11452

5. Harrison, A., Olds-Clarke, P., and King, S. M. (1998) *J. Cell Biol.* 140, 1137–1147

6. Pazour, G. J., Wilkerson, C. G., and Witman, G. B. (1998) *J. Cell Biol.* 141, 979–992

7. Yang, P., Diener, D. R., Rosenbaum, J. L., and Sale, W. S. (2001) *J. Cell Biol.* 153, 1315–1326

8. Dick, T., Ray, K., Salz, H. K., and Chia, W. (1996) *Mol. Cell. Biol.* 16, 1966–1977

9. Puthalakath, H., Huang, D. C., O'Reilly, L. A., King, S. M., and Strasser, A. (1999) *Mol. Cell* 3, 287–296

10. Benashski, S. E., Harrison, A., Patel-King, R. S., and King, S. M. (1997) *J. Biol. Chem.* 272, 20929–20935

11. Liang, J., Jaffrey, S. R., Guo, W., Snyder, S. H., and Clardy, J. (1999) *Nat. Struct. Biol.* 6, 735–740

12. Fan, J., Zhang, Q., Tochio, H., Li, M., and Zhang, M. (2001) *J. Mol. Biol.* 306, 97–108

13. Ghosh-Roy, A., Desai, B. S., and Ray, K. (2005) *Mol. Biol. Cell* 16, 3107–3116

14. Tan, G. S., Preuss, M. A., Williams, J. C., and Schnell, M. J. (2007) *Proc. Natl. Acad. Sci. U.S.A.* 104, 7229–7234

15. Williams, J. C., Roulhac, P. L., Roy, A. G., Vallee, R. B., Fitzgerald, M. C., and Hendrickson, W. A. (2007) *Proc. Natl. Acad. Sci. U.S.A.* 104, 10028–10033

16. Barbar, E. (2008) *Biochemistry* 47, 503–508

17. Vadlamudi, R. K., Bagheri-Yarmand, R., Yang, Z., Balasenthil, S., Nguyen, D., Sahin, A. A., den Hollander, P., and Kumar, R. (2004) *Cancer Cell* 5, 575–585

18. Song, Y., Benison, G., Nyarko, A., Hays, T. S., and Barbar, E. (2007) *J. Biol. Chem.* 282, 17272–17279

19. Song, C., Wen, W., Rayala, S. K., Chen, M., Ma, J., Zhang, M., and Kumar, R. (2008) *J. Biol. Chem.* 283, 4004–4013

20. Huang, B., Piperno, G., Ramanis, Z., and Luck, D. J. (1981) *J. Cell Biol.* 88, 80–88

21. Yang, C., Owen, H. A., and Yang, P. (2008) *J. Cell Biol.* 180, 403–415

22. Harris, H. H. (2009) in *Chlamydomonas* Source Book (Harris, E. H., ed) 2nd Ed., Vol. 1, pp. 242–259, Elsevier Inc., Oxford, UK

23. Lechtreck, K. F., and Witman, G. B. (2007) *J. Cell Biol.* 176, 473–482

24. Yang, P., Diener, D. R., Yang, C., Kohno, T., Pazour, G. J., Dienes, J. M., Agrin, N. S., King, S. M., Sale, W. S., Kamiya, R., Rosenbaum, J. L., and Witman, G. B. (2006) *J. Cell Sci.* 119, 1165–1174

25. Hou, Y., Pazour, G. J., and Witman, G. B. (2004) *Mol. Biol. Cell* 15, 4382–4394

26. Qin, H., Diener, D. R., Geimer, S., Cole, D. G., and Rosenbaum, J. L. (2004) *J. Cell Biol.* 164, 255–266

27. Perrone, C. A., Tritschler, D., Taulman, P., Bower, R., Yoder, B. K., and Porter, M. E. (2003) *Mol. Biol. Cell* 14, 2041–2056

28. Yang, P., and Sale, W. S. (1998) *Mol. Biol. Cell* 9, 3335–3349

29. LeDizet, M., and Piperno, G. (1995) *Mol. Biol. Cell* 6, 697–711

30. DiBella, L. M., Gorbatyuk, O., Sakato, M., Wakabayashi, K., Patel-King, R. S., Pazour, G. J., Witman, G. B., and King, S. M. (2005) *Mol. Biol. Cell* 16, 5661–5674

31. Wirschell, M., Yang, C., Yang, P., Fox, L., Yanagisawa, H. A., Kamiya, R., Witman, G. B., Porter, M. E., and Sale, W. S. (2009) *Mol. Biol. Cell* 20, 3044–3054

32. Kamiya, R. (2002) *Int. Rev. Cytol.* 219, 115–155

33. Wang, W., Lo, K. W., Kan, H. M., Fan, J. S., and Zhang, M. (2003) *J. Biol. Chem.* 278, 41491–41499

34. Rompolas, P., Pedersen, L. B., Patel-King, R. S., and King, S. M. (2007) *J. Cell Sci.* 120, 3653–3665

35. Bower, R., Vanderwaal, K., O'Toole, E., Fox, L., Perrone, C., Mueller, J., Wirschell, M., Kamiya, R., Sale, W. S., and Porter, M. E. (2009) *Mol. Biol. Cell* 20, 3055–3063

36. Hendrickson, T. W., Perrone, C. A., Griffin, P., Wuichet, K., Mueller, J., Yang, P., Porter, M. E., and Sale, W. S. (2004) *Mol. Biol. Cell* 15, 5431-5442

37. Lo, K. W., Kan, H. M., Chan, L. N., Xu, W. G., Wang, K. P., Wu, Z., Sheng, M., and Zhang, M. (2005) *J. Biol. Chem.* 280, 8172–8179

38. Rodríguez-Crespo, I., Ye´lamos, B., Roncal, F., Albar, J. P., Ortiz de Montellano, P. R., and Gavilanes, F. (2001) *FEBS Lett.* 503, 135–141

39. Lo, K. W., Kan, H. M., and Pfister, K. K. (2006) *J. Biol. Chem.* 281, 9552–9559

40. Delanoue, R., Herpers, B., Soetaert, J., Davis, I., and Rabouille, C. (2007) *Dev. Cell* 13, 523–538

41. Jaffrey, S. R., and Snyder, S. H. (1996) *Science* 274, 774–777

FIGURE 1. *pf5* strain, CC1331, has multiple flagellar defects. *A,* most CC1331 cells (CC1331; *bottom panel*) are stationary with paralyzed or twitching flagella that are one-half the length of wild-type flagella (*WT*; *upper panel*). On occasion, flagella of unequal lengths (*arrowhead*) and flagella with swollen tips (*arrow* in *insets*) are observed. *B,* Western blots of isolated axonemes reveal defects in I1 dynein and the RS in CC1331. Different loads of axonemes were included to better reveal the reduction level. The I1-dynein subunit, IC97, is undetectable, whereas the WD repeat subunit, IC140, appears normal. Two representative radial spoke proteins, RSP3 and RSP16, are reduced to less than 50% of the WT level, and the dephosphorylated form of RSP3 is more prominent in CC1331 (*lower band* in *CC1331 RSP3 lane*). IC78, LC6, and LC9 in the ODA, DLIC in CD1b, and p28 (a component of several single-headed IDAs) appear normal.

Journal of Biological Chemistry, Vol. 284, No. 45 (November 2009): pg. 21412-31421. DOI.

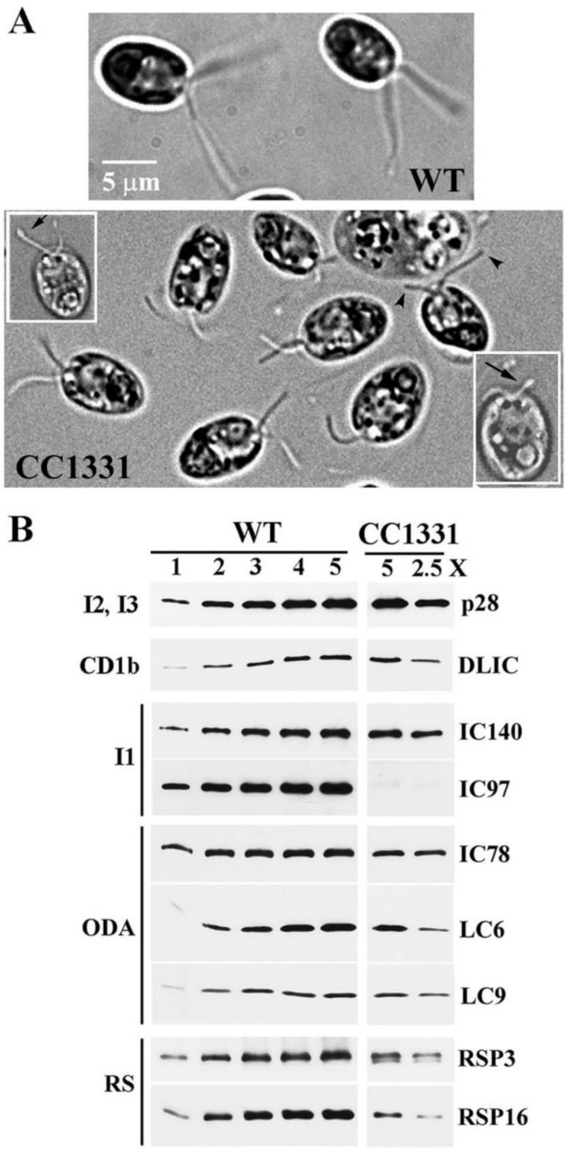

TABLE 1
Characteristics of LC8 mutants

	LC8 *in vitro*	Flagella length	Motility	Beat frequency	ODA	I1	RS
fla14-1 (null)[a]	NA[b]	Shortest	Immotile	NA	Absent	Reduced	Absent
CC1331 (LC8CT) *fla14-3*	Dimer[c]	Shorter	Immotile, twitching	NA	Normal	IC97 −, unstable	Reduced, dephosphorylated RSP3 unstable
fla14-LC8S90E	Monomer	Normal	WT to *oda*-like	~50–60 Hz	Reduced LC6, LC9 unstable	IC97 −	Normal
fla14-LC8S90A	Dimer[c]	Normal	WT	~60 Hz	Normal	Normal	Normal
fla14-LC8 (WT)	Dimer	Normal	WT	~60 Hz	Normal	Normal	Normal

[a] Data reported by Pazour *et al.* (6).
[b] NA means not applicable.
[c] Data reported by Song *et al.* (18).

FIGURE 2. CC1331 phenotype is because of a read-through mutation in the LC8 gene. *A,* motility and Western blots of isolated axonemes from representative progeny derived from a cross between CC1331 and WT reveal only parental di-type tetrads, twitching flagella (*T*) characteristic of the CC1331 phenotype and wild-type swimming cells (*S*). The phenotypes, including twitching short flagella (*T*), dephosphorylated RSP3 (*dot*), and the absence of IC97, strictly co-segregate. *B,* comparison of the C-terminal sequences of LC8 in CC1331 and WT. The stop codon in the LC8 gene is mutated into a leucine codon (*asterisk*), resulting in the addition of 23 amino acids at the C terminus. This C-terminal extension may alter the original 5th β-strand into a helix (*h*). *C,* Western blot shows that the LC8 with a C-terminal extension (LC8CT) is present in CC1331 axoneme and slightly larger than WT LC8. The *middle lane* contains both WT and CC1331 axonemes. *D,* representative Western blots show that the WT LC8 gene rescues the motility and axonemal deficiencies of CC1331. In the axonemes of the transformants, WT LC8 co-assembles with the larger endogenous LC8CT. The ratio of WT:LC8CT correlates with the percentage of swimmers and the amount of IC97 and phosphorylated RSP3. Interestingly, 50% assembly of WT LC8 rescues the flagellar phenotypes (B1). Like the CC1331 parental strain, the CC1331-like strains (H8, G1, and H7) yield less axonemes (see tubulin protein stain), but dephosphorylated RSP3 (*dot*), typical of CC1331 axonemes, is still observed.

NOT THE PUBLISHED VERSION; this is the author's final, peer-reviewed manuscript. The published version may be accessed by following the link in the citation at the bottom of the page.

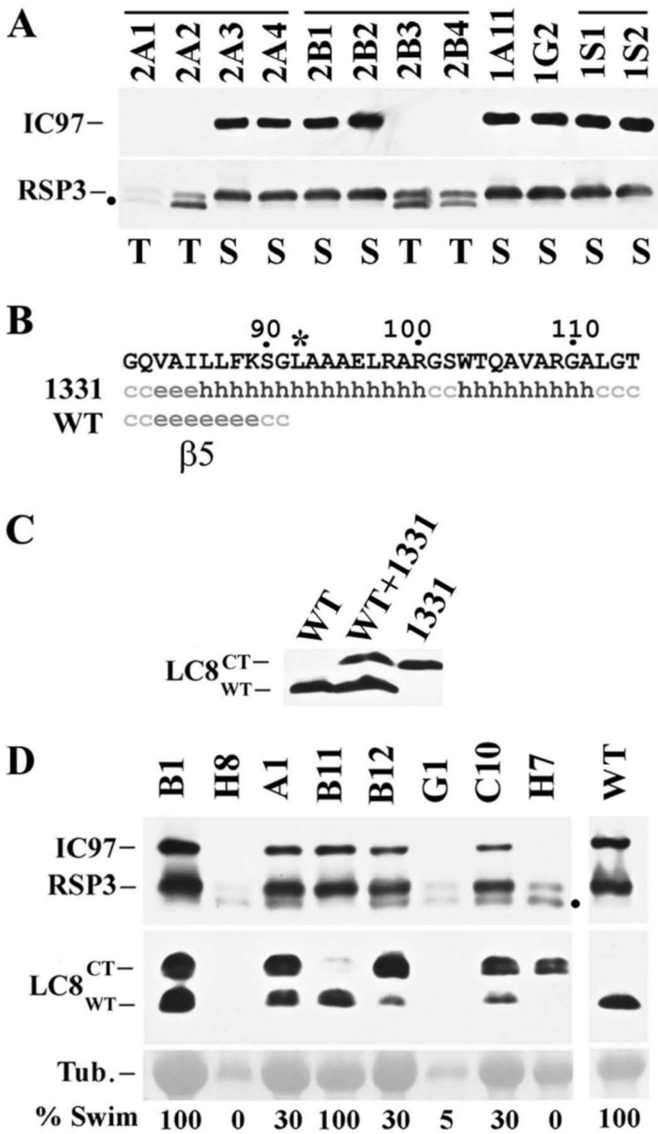

Journal of Biological Chemistry, Vol. 284, No. 45 (November 2009): pg. 21412-31421. DOI.

FIGURE 3. Two C-terminal mutations affect LC8 dimerization differently. *A,* tertiary structure modeling illustrates the location of Ser^{88} (*yellow residues* with side chains) and the C terminus near the dimeric interface. The diagram is based on the NMR study of the rat LC8 dimer (*blue* and *green*) and Bim peptide (*pink*) (12) and was generated by the web-based program, Protein Data Bank Workshop 1.50. *B,* gel filtration shows that at pH 7 LC8CT migrates as a larger particle than dimericWTLC8 and the monomeric phosphomimetic LC8S90E (*upper panel*). In contrast, at pH 3, all LC8 forms migrate primarily as monomers (*bottom panel*).

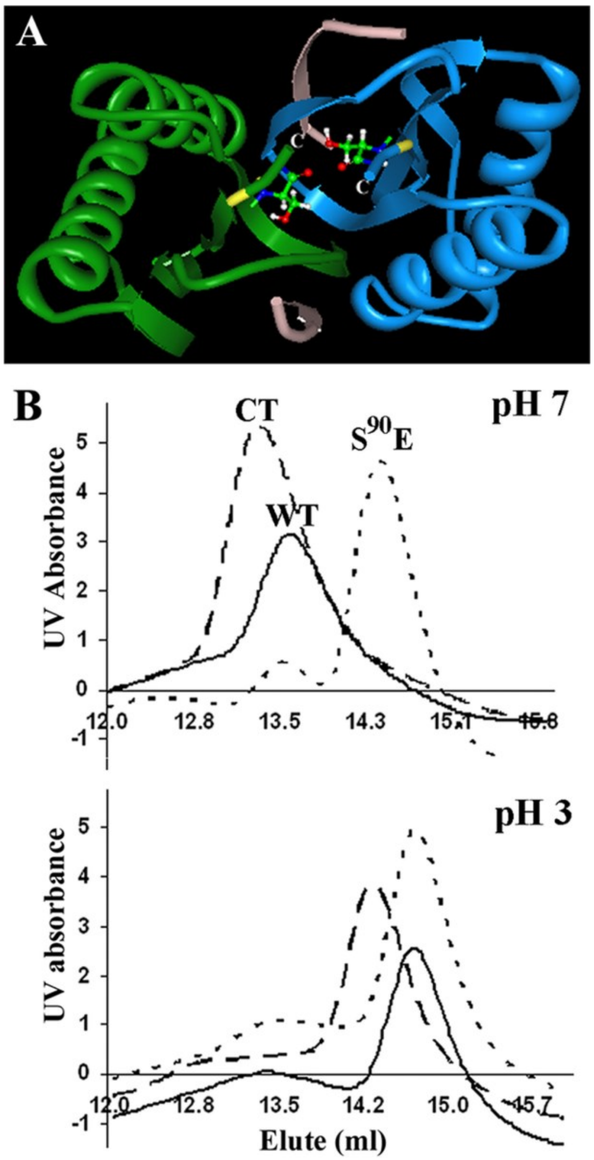

FIGURE 4. S90E mutation in *Chlamydomonas* LC8 results in subtle phenotypes. For these experiments, *fla14-1* was transformed with constructs to express LC8, LC8CT, LC8S90E, and LC8S90A. *A,* flagellar lengths of the transformants expressing LC8 variants. Each data point was obtained from measuring 100 flagellated cells from each transformant at different time points after the beginning of the light cycle. As expected, the WT LC8 transformant has full-length flagella (LC8) and the LC8CT transformant has short flagella that are about one-half the length of wild type and slightly longer than that of *fla14-1*. The transformants expressing the LC8S90E protein are full-length (S90E). *CT*, C terminus. *B,* Western blot of axonemes treated with increasing concentrations of 1,5-difluoro-2,4-dinitrobenzene shows that LC8S90E is cross-linked into a dimer as effectively as WT LC8 (*arrowhead*). *C,* Western blots of isolated axonemes demonstrate IC97 from I1 is absent, and LC6 and LC9 from ODA are reduced in axonemes from LC8S90E transformants (*lanes #17*, *#8*, and *#2*). RS assembly appears normal (RSP3 and RSP16). IC140 and p28 are unaffected and thus serve as loading controls. *D,* differences between LC8S90E transformants and the control, LC8S90A, and WT become obvious when cultured in a dimly lighted 32 °C room. The *histogram* shows the percentage of swimmers after resuspension of cells from agar plate. Note under this condition, 10–50% of the cells in the control groups can swim after 0.5–3 h, compared with ~100% in the standard laboratory condition. However, only ~10% LC8S90E becomes motile after 3.5 h. Cell numbers counted from five randomly chosen fields were averaged and rounded off to reflect the approximate assessment of moving cells.

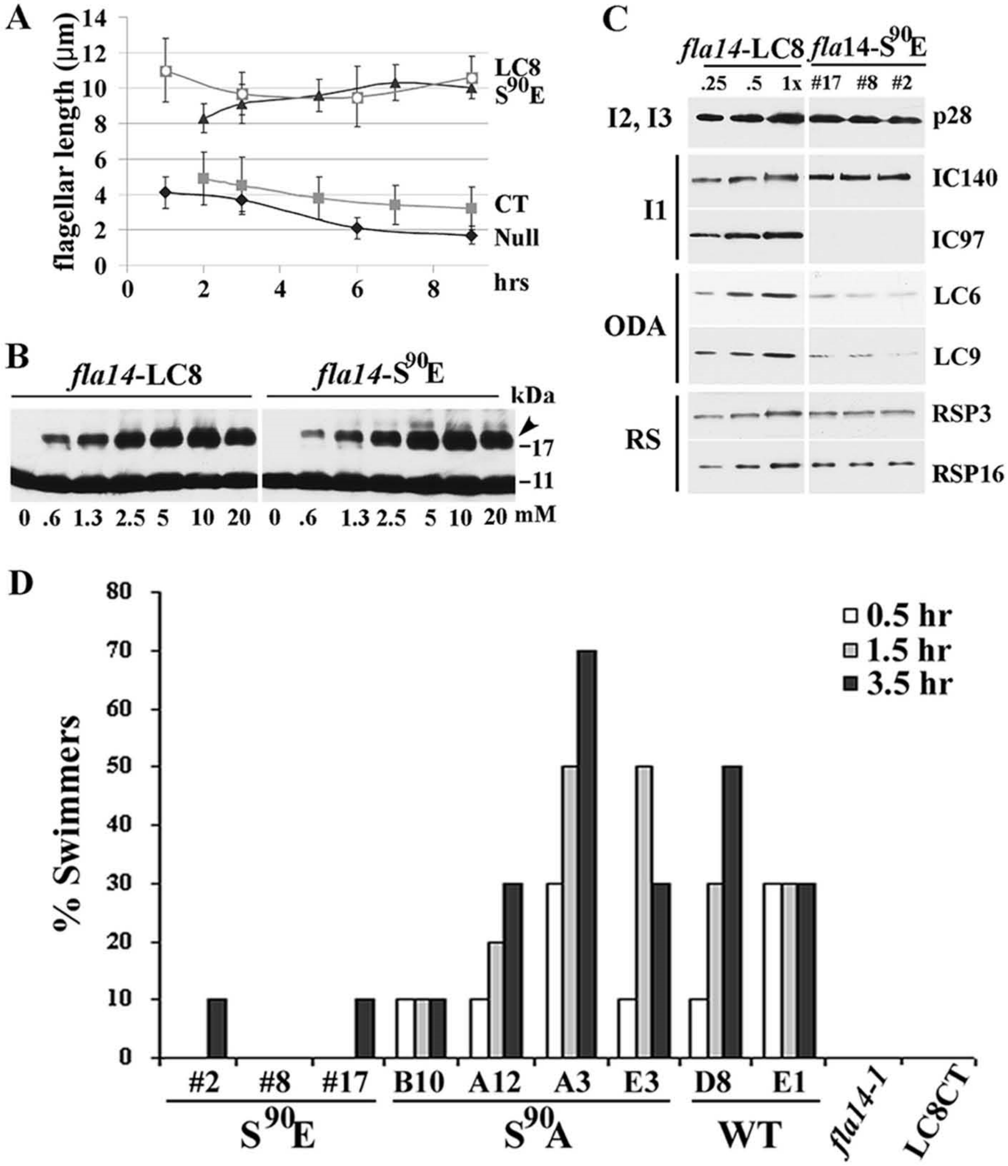
A
flagellar length (μm)
hrs
LC8
S90E
CT
Null
B
fla14-LC8
fla14-S90E
kDa
-17
-11
0 .6 1.3 2.5 5 10 20 0 .6 1.3 2.5 5 10 20 mM
C
fla14-LC8
fla14-S90E
.25 .5 1x #17 #8 #2
I2, I3
p28
I1
IC140
IC97
ODA
LC6
LC9
RS
RSP3
RSP16
D
% Swimmers
0.5 hr
1.5 hr
3.5 hr
#2 #8 #17 B10 A12 A3 E3 D8 E1
S90E
S90A
WT
fla14-1
LC8CT

FIGURE 5. Differential instability of axonemal complexes in each LC8 mutant. Axonemal complexes were extracted by NaCl (*A*) or KI (*B*) buffer and separated by velocity sedimentation through a 5–20% sucrose gradient. The gradient fractions were analyzed by Western blots. *A,* differential dissociation of ODA and I1. The ODA and I1 dynein from WT LC8 axonemes represented by IC78 and IC140, respectively, sediment at ~20 S (*arrowhead*). LC8 primarily co-sediments with the ODA. In an LC8CT transformant (CC1331 as well, not shown), I1 dissociates; both IC138 and IC140 sediment as distinct smaller particles. In contrast, the ODA remain intact at ~20 S. *Arrow* indicates the p28 peak for single-headed dyneins. In the LC8S90E gradient, the ODA dissociates; both IC78 and IC69 sediment as distinct particles (*arrowheads* in IC78 and IC69 panels), whereas I1 remains stable (*arrowhead* in IC140 panel). LC8 largely co-sediments with IC69 of the ODA (*arrowhead* in LC8 panel). The LC8S90A gradient is similar to that of WT. *B,* RS from LC8CT axonemes dissociate upon extraction. Represented by RSP16, the RS in *fla14*-LC8, *fla14*-LC8S90E, and *fla14*-LC8S90A extracts sediments as an ~20 S particle. In contrast, RSPs extracted from LC8CT strains sediment near the top of the gradient indicating a drastic dissociation of the RS complex.

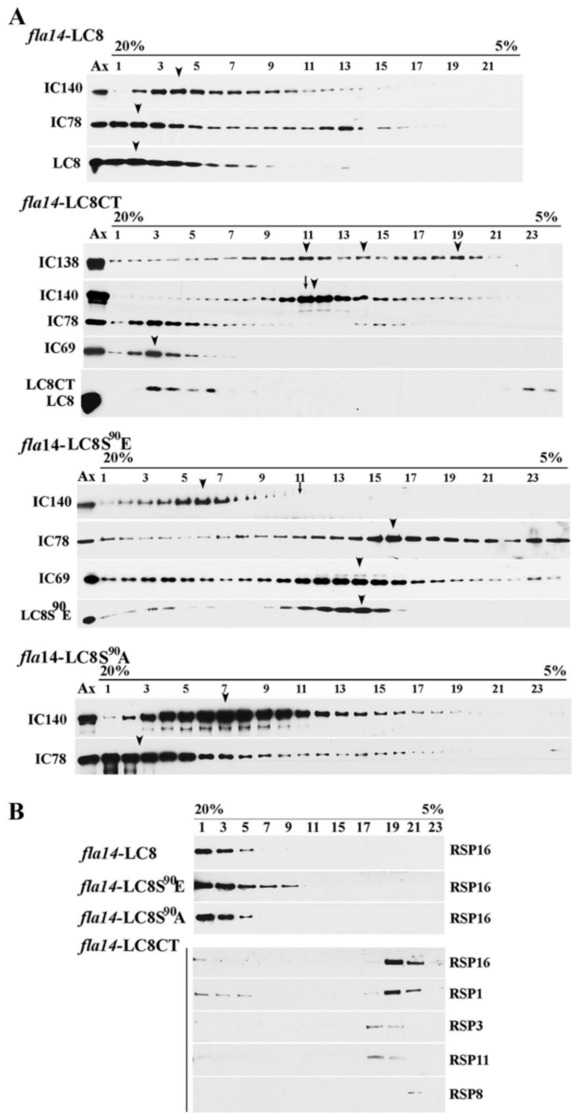
A
fla14-LC8
20%
5%
IC140
IC78
LC8
fla14-LC8CT
IC138
IC140
IC78
IC69
LC8CT
LC8
fla14-LC8S90E
IC140
IC78
IC69
LC8S90E
fla14-LC8S90A
IC140
IC78
B
fla14-LC8
fla14-LC8S90E
fla14-LC8S90A
fla14-LC8CT
RSP16
RSP1
RSP3
RSP11
RSP8

FIGURE 6. Model explaining the influence of dimeric LC8 and LC8CT on molecular complexes. Binding of the WT LC8 dimer (*left*) to the disordered regions (*squiggly lines*) of target proteins (such as the dynein ICs) induces refolding and thus promotes the association of additional subunits, *e.g.* IC97 in I1 dynein and the LC6 dimer in ODA. Mutant LC8 (LC8CT, *right*) binds to its target proteins (the ICs), but the additional C-terminal tails at the interface (*triangles*) interfere with the proper structural changes required for recruiting IC97. Binding of the LC6 dimer is not affected by this mutation and thus no impact on the ODA is observed. The inherent differences among scaffold proteins and flanking molecules may determine the differential effects of LC8 modifications, including phosphorylation.

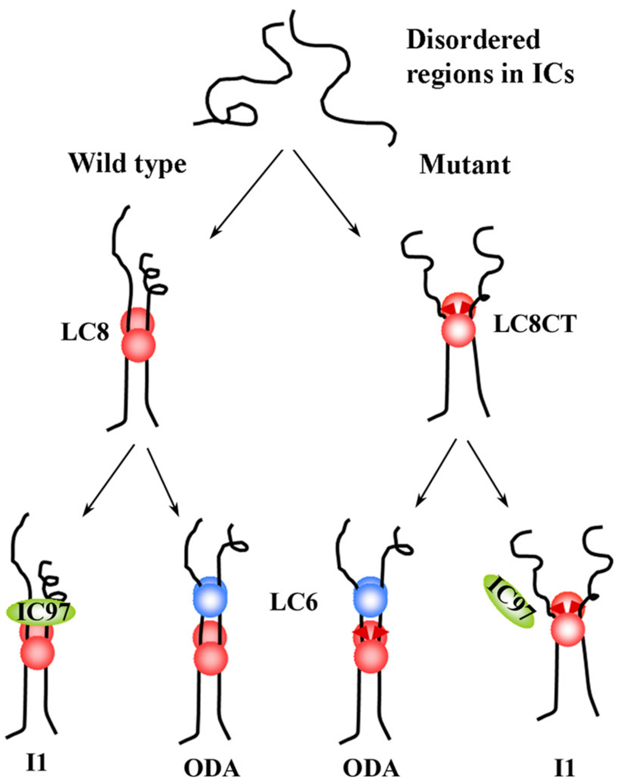

* This work was supported, in whole or in part, by National Institutes of Health Grant GM068101 (to P. Y.) and National Research Service Award Postdoctoral Fellowship GM075446 (to M. W.).

[1] Both authors contributed equally to this work.

[2] To whom correspondence should be addressed: 530 N. 15th St., Milwaukee, WI 53233. Tel.: 414-288-5663; Fax: 414-288-7357; E-mail: pinfen.yang@marquette.edu.

[3] The abbreviations used are: ODA, outer dynein arms; RS, radial spokes; DLIC, dynein light intermediate chain; IDA, inner dynein arms; IFT, intraflagellar transport; PMM, paromomycin; WT, wild type.

